UNIVERSIDAD REGIONAL AMAZÓNICA IKIAM

FACULTAD DE CIENCIAS DE LA TIERRA Y AGUA

CARRERA DE GEOCIENCIAS

ANÁLISIS ESPACIAL DE LA SUSCEPTIBILIDAD A DESLIZAMIENTOS DE TIERRA EN LA VÍA TENA–PAPALLACTA: APLICACIÓN DEL MÉTODO DE MORA-VARHSON Y DATOS CLIMÁTICOS HISTÓRICOS

Proyecto de investigación previo a la obtención del Título de:

INGENIERO EN GEOCIENCIAS

AUTOR

JOSUÉ DANIEL CAMPUZANO GOYA

Tena - Ecuador

2025

UNIVERSIDAD REGIONAL AMAZÓNICA IKIAM

FACULTAD DE CIENCIAS DE LA TIERRA Y AGUA

CARRERA DE GEOCIENCIAS

ANÁLISIS ESPACIAL DE LA SUSCEPTIBILIDAD A DESLIZAMIENTOS DE TIERRA EN LA VÍA TENA–PAPALLACTA: APLICACIÓN DEL MÉTODO DE MORA-VARHSON Y DATOS CLIMÁTICOS HISTÓRICOS

Proyecto de investigación previo a la obtención del Título de:

INGENIERO EN GEOCIENCIAS

AUTOR: JOSUÉ DANIEL CAMPUZANO GOYA

TUTOR: MSc. JORGE RONNY ESPÍN CAMPOS

Tena - Ecuador

2025

Carrera de Geociencias

Declaración de derecho de autor, autenticidad y responsabilidad

Tena, 07 de marzo de 2025

Yo, Josué Daniel Campuzano Goya con documento de identidad 2200080733, declaro que los resultados obtenidos en la investigación que presento en este documento final, previo a la obtención del título Ingeniero en Geociencias, son absolutamente inéditos, originales, auténticos y personales.

En virtud de lo cual, el contenido, criterios, opiniones, resultados, análisis, interpretaciones, conclusiones, recomendaciones y todos los demás aspectos vertidos en el presente documento, son de mi autoría y de mi absoluta responsabilidad.



Josué Daniel Campuzano Goya
CI: 2200080733

Carrera de Geociencias

Autorización de publicación en el repositorio institucional

Tena, 07 de marzo de 2025

Yo, Josué Daniel Campuzano Goya, con documento de identidad 2200080733 en calidad de autor/a y titular de los derechos morales y patrimoniales del trabajo de titulación "Análisis espacial de la susceptibilidad a deslizamientos de tierra en la vía Tena–Papallacta: Aplicación del método de Mora-Varhson y datos climáticos históricos" de conformidad con el Art. 114 del CÓDIGO ORGÁNICO DE LA ECONOMÍA SOCIAL DE LOS CONOCIMIENTOS, CREATIVIDAD E INNOVACIÓN, reconozco a favor de la Universidad Regional Amazónica Ikiam una licencia gratuita, intransferible y no exclusiva para el uso no comercial de la obra, con fines estrictamente académicos.

Así mismo autorizo a la Universidad Regional Amazónica Ikiam para que realice la publicación de este trabajo de titulación en el Repositorio Institucional de conformidad a lo dispuesto en el Art. 144 de la Ley Orgánica de Educación Superior.



Josué Daniel Campuzano Goya
CI: 2200080733

Carrera de Geociencias

Certificado de dirección de trabajo de titulación

Tena, 07 de marzo de 2025

Certifico que el trabajo de titulación: “Análisis espacial de la susceptibilidad a deslizamientos de tierra en la vía Tena–Papallacta: Aplicación del método de Mora-Varhson y datos climáticos históricos”, aprobado bajo el mecanismo de titulación de: artículo, fue realizado por Josué Daniel Campuzano Goya, bajo mi dirección.

El mismo ha sido revisado en su totalidad y analizado por la herramienta de verificación de similitud de contenido; por lo tanto, cumple con los requisitos teóricos, científicos, técnicos, metodológicos y legales establecidos por la Universidad Regional Amazónica Ikiam, para su entrega y defensa.

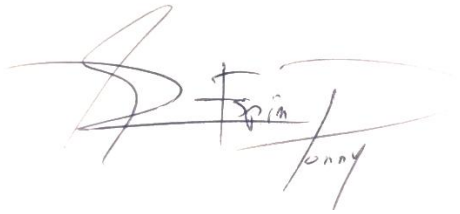

MSc**.** Jorge Ronny Espín Campos
C.I: 1600488207
Tutor

AGRADECIMIENTOS

Gracias a quienes hicieron posible mi formación y crecimiento personal. Primero, a mis padres, Ecuador y Virginia, mi mayor inspiración en la vida. Les agradezco infinitamente su amor incondicional, sus sabios consejos, su paciencia infinita y todo el apoyo que me han brindado a lo largo de los años. Gracias por trabajar incansablemente para que pudiera estudiar y por enseñarme a luchar por mis sueños sin rendirme jamás. A mis hermanas, Sharon y Camila, y a mi adorable sobrino Nicolás, la alegría de nuestras vidas, gracias por sus inmensos abrazos y por hacerme sentir siempre querido.

También quiero agradecer a mi tutor, Ronny Espín, por la confianza depositada en mí, por su guía, sus consejos y las oportunidades que me brindó para crecer profesionalmente. A los profesores Corina Campos y Oswaldo Guzmán, les estoy en deuda por su conocimiento compartido, por sus inspiradoras charlas y por las oportunidades que me brindaron durante mi formación. Agradezco a todos los docentes que compartieron sus conocimientos conmigo, en especial a los de la Facultad de Ciencias de la Tierra y Agua, quienes con sus enseñanzas me llevaron a amar las Geociencias.

Al amor de mi vida, Milena, gracias por tu apoyo incondicional, especialmente cuando sentía que me ahogaba en un vaso de agua. Tu apoyo fue fundamental para superar los desafíos. Ehiner gracias por tu amistad sincera y por todos los momentos inolvidables que hemos compartido durante nuestra vida universitaria, nunca olvidaré la primera vez que nos vimos después de las largas charlas por videollamada. Espero que nuestra amistad perdure para siempre.

Finalmente, agradezco a Dios por la vida, por la oportunidad de aprender y crecer rodeado de personas tan maravillosas.

DEDICATORIA

Con todo mi amor y gratitud, dedico este trabajo de investigación a mis padres, Ecuador y Virginia, pilares de mi vida, por su amor incondicional, su paciencia infinita y por creer en mí en cada paso del camino. A mis hermanas, Sharon y Camila, y a mi querido sobrino, Nicolas, por llenar mis días de alegría y por su constante apoyo. A mi enamorada Milena, por su comprensión, su amor y por estar a mi lado en cada momento.

A mis docentes, quienes me inspiraron a amar las Geociencias y me guiaron en este camino de aprendizaje, por su apoyo y confianza. A mis amigos, por los recuerdos inolvidables y los momentos de alegría que compartimos, y a todas las personas que me motivaron a lo largo de esta etapa de mi vida. Este logro es también suyo.

TABLA DE CONTENIDO

PORTADA
Declaración de derecho de autor, autenticidad y responsabilidad i
Autorización de publicación en el repositorio institucional ii
Certificado de dirección de trabajo de titulación iii
AGRADECIMIENTOS iv
DEDICATORIA v
TABLA DE CONTENIDO vi
INDICE DE TABLAS vii
ÍNDICE DE FIGURAS viii
RESUMEN x
ABSTRACT xi
1 Introduction 1
1.1 Study Area 2
1.2 Geological Setting 4
2 Methods 6
2.1 Passive factors 7
2.1.1 Relative relief (Sr) 7
2.1.2 Lithology (Sl) 10
2.1.3 Soil Moisture (Sh) 13
2.2 Triggering Factors 14
2.2.1 Seismicity (Ts) 14
2.2.2 Precipitation intensity (Tp) 16
3 Results and Discussions 23
3.1 Passive factors 23
3.1.1 Relative relief (Sr) 23
3.1.2 Lithology (Sl) 24
3.1.3 Soil Moisture (Sh) 26
3.2 Triggering Factors 27
3.2.1 Seismicity (Ts) 27
3.2.2 Precipitation intensity (Tp) 29
4 Conclusions 35
References

INDICE DE TABLAS

Table 1. Landslide Susceptibility Variables..... 6

Table 2. Morphometric classification..... 9

Table 3. Classification of different lithologies and their susceptibilities. 11

Table 4. Classification of average monthly values of rainfall. 13

Table 5. Meteorological Stations 17

Table 6. Pmax values in mm/day recorded from 1971 to 2013 at the meteorological stations. 19

Table 7. Rainfall intensity factor (Tp) resulting from the classification of maximum daily rainfall for a return period of 100 years and 10 years or less. 21

Table 8. Calculation of the 100-year return period rainfall intensity in mm/day 29

ÍNDICE DE FIGURAS

Figure 1. Location of the study area. The road is depicted as a black line, traversing a varied altitudinal range, indicated by the meters above sea level (m.a.s.l.) scale. The city of Tena, in the Ecuadorian Amazon, is located in the south of the map, while Papallacta, positioned in the Ecuadorian Andes, is located in the northwest..... 3

Figure 2. Geological map of Ecuador based on Égüez et al. (2017), showing only the geologica formations through which the road crosses. In addition, the locations of landslides inventoried by Espín et al. (2018) are shown. 5

Figure 3. Shows the seismic zonation map of Ecuador, which defines different seismic zones based on ground acceleration values, as established in the Normativa Ecuatoriana de la Construcción NEC-11 (2015). 15

Figure 4. Map of the location of the meteorological stations used for the calculation of precipitation intensity..... 18

Figure 5. Relative Relief Maps for the Tena-Papallacta Road. (A) Vertical dissection (Dv) classified into 11 levels. (B) Relative relief (Sr) classified according to the Mora-Varshson methodology. 23

Figure 6. Lithology map (Sl) for the Tena-Papallacta road, classified according to the Mora-Varshson methodology..... 25

Figure 7. Precipitation maps for the Tena-Papallacta road. (A) Historical precipitation record (1985–2015) in raster format. (B) Mean monthly precipitation map (Sh) classified according to the Mora–Varshson methodology. 26

Figure 8. Ground acceleration map (Ts) for the Tena-Papallacta road, showing the classification in relation to influence. 28

Figure 9. Precipitation intensity maps for the Tena-Papallacta road. (A) Rainfall intensity with a 100-year return period, obtained through IDW interpolation. (B) Rainfall intensity map (Tp) classified according to the Mora-Varshson methodology. 30

Figure 10. Landslide susceptibility maps for the Tena-Papallacta road. (A) Final susceptibility obtained using the Mora-Varshson method, incorporating both triggering factors (seismicity and precipitation intensity). (B) Susceptibility derived considering only seismicity as a triggering factor. (C) Susceptibility calculated including only precipitation intensity as a triggering factor. 34

RESUMEN

La vía Tena-Papallacta, vital para la conexión entre la Amazonía y los Andes ecuatorianos, ya que facilita el transporte de bienes, servicios y personas entre estas dos regiones, ha sufrido fenómenos de remoción en masa, principalmente por su compleja geografía, litología susceptible y la frecuencia de lluvias torrenciales. El presente estudio permite a lo largo de la vía Tena–Papallacta categorizar por tramos sitios susceptibles a sufrir fenómenos de remoción en masa. Se utilizó el método de Mora-Varhson, que incluye capas de relieve relativo, litología y humedad del suelo como factores pasivos, y sismicidad e intensidad de precipitación como factores detonantes, junto con datos climáticos históricos, para generar información que se representó en un sistema de información geográfica. El análisis identificó una muy alta susceptibilidad entre Papallacta y Baeza, susceptibilidad media a alta entre Baeza y la "Y" de Narupa, y susceptibilidad media a muy baja entre la "Y" de Narupa y Tena. La validación del modelo con un inventario de deslizamientos confirmó su precisión del 97.37% en la predicción de fenómenos de remoción en masa presentes en las clases 4 y 5. Este estudio da información crucial para la gestión del riesgo a deslizamientos en la zona, que puede utilizarse para planificar medidas de mitigación.

Palabras clave: Amazonía, Deslizamientos, Inventario, Susceptibilidad, Vía.

ABSTRACT

The Tena-Papallacta road, a vital link between the Amazon Region and the Ecuadorian Andes, facilitates the transport of goods, services and people between these regions. However, it has experienced frequent mass wasting events, primarily due to its complex geography, susceptible lithology, and the prevalence of torrential rainfall. This study assessed landslide susceptibility along the Tena-Papallacta road, categorizing segments based on their susceptibility to mass wasting. The Mora-Varshson method was employed, incorporating layers of relative relief, lithology, and soil moisture as passive factors, and seismicity and rainfall intensity as triggering factors. Historical climate data was also integrated into the analysis, and the resulting information was represented within a geographic information system (GIS). The analysis identified very high susceptibility between Papallacta and Baeza, moderate to high susceptibility between Baeza and the "Y" de Narupa junction, and moderate to very low susceptibility between the "Y" de Narupa and Tena. Validation of the model using a landslide inventory confirmed its accuracy, with 97.37% of the inventoried landslides falling within the high and very high susceptibility classes (4 and 5). This study provides crucial information for landslide risk management along the Tena-Papallacta road, which can be used to inform mitigation strategies and land-use planning.

Keywords: Amazon Region, Landslides, Inventory, Susceptibility, Road.

Revista: Natural Hazards and Earth System Sciences (NHESS)
Link: NHESS - Home

ANÁLISIS ESPACIAL DE LA SUSCEPTIBILIDAD A DESLIZAMIENTOS DE TIERRA EN LA VÍA TENA–PAPALLACTA: APLICACIÓN DEL MÉTODO DE MORA-VARHSON Y DATOS CLIMÁTICOS HISTÓRICOS

SPATIAL ANALYSIS OF LANDSLIDE SUSCEPTIBILITY ALONG THE TENA-PAPALLACTA ROAD: APPLICATION OF THE MORA-VARSHSON METHOD AND HISTORICAL CLIMATE DATA

Josué Daniel Campuzano Goya[1]*

[1]Universidad Regional Amazónica Ikiam, Parroquia Muyuna, Kilómetro 7 vía a Alto Tena, s/n, Tena, Napo, Ecuador.

*Autor para correspondencia: josue.campuzano@est.ikiam.edu.ec

1 Introduction

The Tena–Papallacta road, a critical route for connectivity between Ecuador's Amazonian and Andean regions, traverses a geographically complex area that is highly susceptible to landslides (Gobierno Provincial de Napo, 2020; Servicio Nacional de Gestión de Riesgos y Emergencias, 2022). These recurrent events have caused significant damage to infrastructure, interruptions to transportation, and even loss of human lives. National press reports highlight notable occurrences, including the July 2024 debris flow in the Maspa sector, which triggered two landslides leading to the closure of the road, and the May 2021 landslide in the Arrayán sector, where a vehicle was buried (El Universo, 2024; El Comercio, 2021). In December 2019, two landslides in the Guacamayos sector resulted in one fatality and thirteen injuries (El Comercio, 2019). Similarly, in July 2015, seven landslides in the Cuyuja sector caused four fatalities and 36 injuries, complicating rescue efforts (El Comercio, 2015). Additionally, a landslide damaged the bridge over the Victoria River, leading to its collapse and interrupting traffic for several days (Secretaría Nacional de Gestión de Riesgos, n.d.).

Landslide susceptibility, defined as the spatial probability of occurrence in a specific location, reflects the propensity of an area to experience such events at both local and regional scales (Brabb, 1984; Hearn and Hart, 2019). Susceptibility models provide an estimate of "where" landslides are expected to occur (Guzzetti et al., 2005). These models play a crucial role in land-use planning and risk management (Aristizabal & Hermelin, 2011; Barrantes, 2010).

Landslides, also referred to as mass movement processes (MMPs), are natural phenomena involving the downslope displacement of soil, rock, or sediment under the influence of gravity. These events contribute to erosion and landscape evolution and can be triggered by various factors, both natural and anthropogenic. Climatic factors, such as intense rainfall and seismic activity, play a crucial role in triggering landslides. Intense rainfall can saturate soil, increase pore water pressure, and reduce the shear strength of slopes, leading to instability and landslides (Nguyen et al., 2020; Yin et al., 2023). Seismic activity can further destabilize slopes and trigger mass movements, particularly

in areas with steep gradients and susceptible geological materials (Alvarado et al., 2014) Therefore, understanding and incorporating historical climate data, including rainfall patterns and and seismicity, is essential for comprehensive landslide susceptibility assessment and risk management.

Numerous methods exist for landslide susceptibility assessment, including the Analytical Hierarchy Process (AHP) proposed by Saaty (1987). However, the Mora-Varshson method (1991, 1994) stands out due to its relative simplicity, its ability to integrate both conditioning and triggering factors, and its effectiveness in identifying landslide-prone areas (Román & Feoli-Boraschi, 2018; López et al., 2020). This method, based on the combination of intrinsic and external factors, is readily integrated with Geographic Information Systems (GIS) for spatial analysis and process modeling (Althuwaynee & Prahan, 2017; Selehpour Jam et al., 2021).

This research aims to evaluate landslide susceptibility along the Tena-Papallacta road using the Mora-Varhson method. To achieve this objective, the study seeks to analyze the influence of factors contributing to landslides, generate a susceptibility map highlighting areas of higher risk, and validate this map through an existing landslide inventory.

1.1 Study Area

The study area encompasses an approximately 124-kilometerroad corridor connecting the cities of Tena and Papallacta across the Amazon Region and Andean regions of Ecuador (Figure 1). This corridor traverses a geographically complex region, transitioning from the Amazonian lowlands to the eastern foothills of the Andes Mountains, resulting in significant variability in topography, geology, and climate.

Tena–"Y" de Narupa segment (E45) crosses the Amazonian landscape, which is characterized by a humid tropical climate and moderate slopes. From the "Y" de Narupa to Baeza (E20–E45), the road ascends a significant altitudinal gradient, entering the Andean region with steep slopes and increased precipitation. The Baeza to Papallacta

segment (E20) traverses a high-mountain Andean environment marked by extreme climatic conditions, where the geological characteristics and climatic variability contribute to the frequent occurrence of mass-wasting processes (Ministerio del Ambiente de Ecuador, 2014; Dirección Nacional de Geología, 2002).

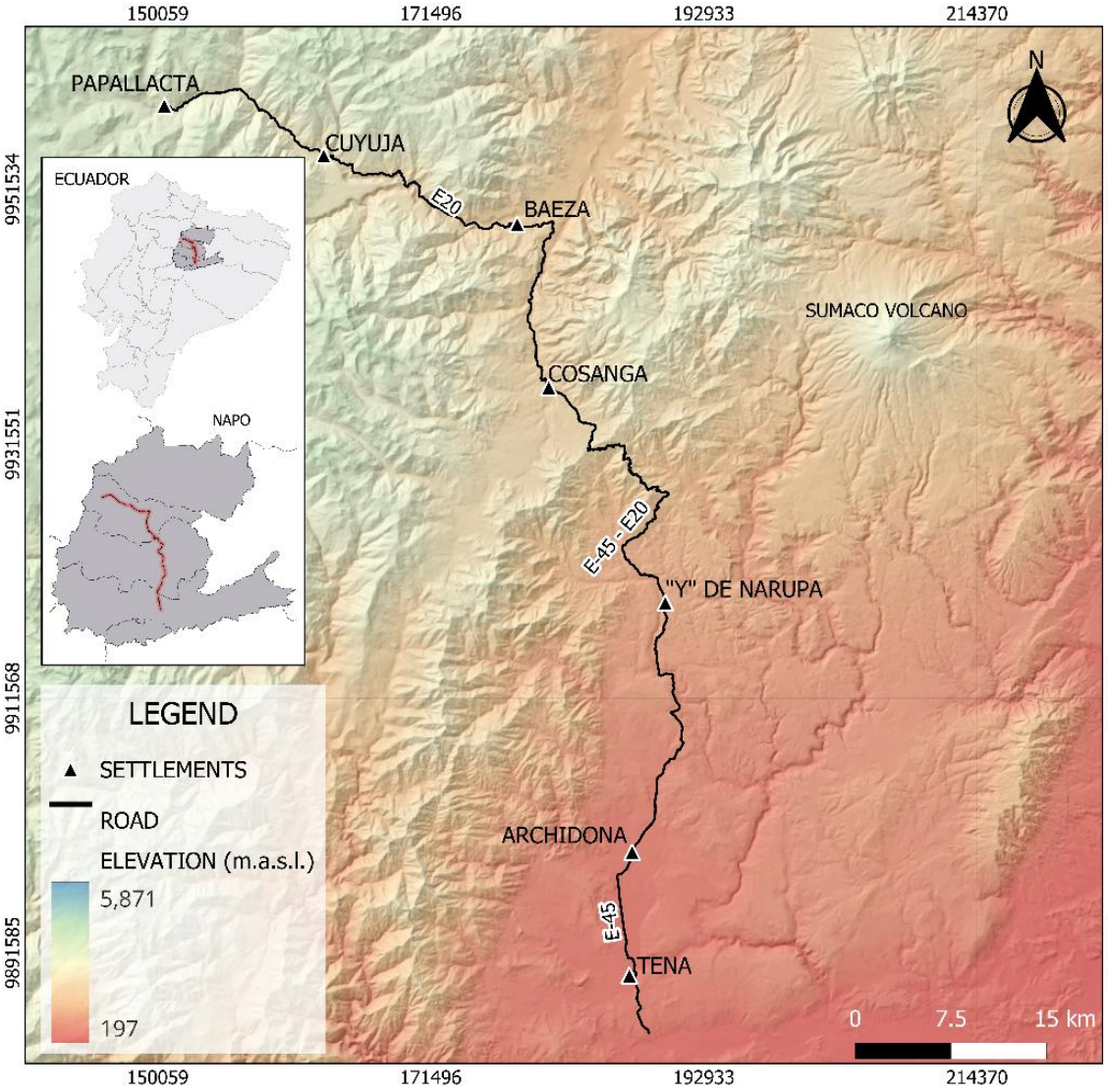

Figure 1. Location of the study area. The road is depicted as a black line, traversing a varied altitudinal range, indicated by the meters above sea level (m.a.s.l.) scale. The city of Tena, in the Ecuadorian Amazon, is located in the south of the map, while Papallacta, positioned in the Ecuadorian Andes, is located in the northwest.

1.2 Geological Setting

The Tena-Papallacta road traverses a diverse geological landscape, encountering a variety of Formations along its path. From Tena to the "Y" de Narupa, the road crosses the Tena, Napo, and Hollín Formations. Between Narupa and Cosanga, the road intersects the Misahuallí Unit, the Abitagua Granite, alkaline basaltic lavas from Sumaco Volcano, and the Napo Formation. From Cosanga to Baeza, the Tena and Napo Formations are prevalent. Finally, the segment from Baeza to Papallacta is dominated by the Upano, Cuyuja, and Chiguinda (Loja) units, along with the Tres Lagunas and Agoyán Units, and the Chacana Volcano caldera (Egüez et al., 2017).

The road alignment crosses 14 Geological Formations, composed mainly of lutites, limestones, sandstones (quartzose and calcareous), volcanic rocks, volcanic breccias, tuffs, agglomerates, gneisses, deformed granites, schists, black phyllites, and quartzites. In addition, Quaternary deposits are identified, among which alkaline basaltic lavas and avalanche debris stand out (Egüez et al., 2017; Núñez, 2003; Baldock, 1982).

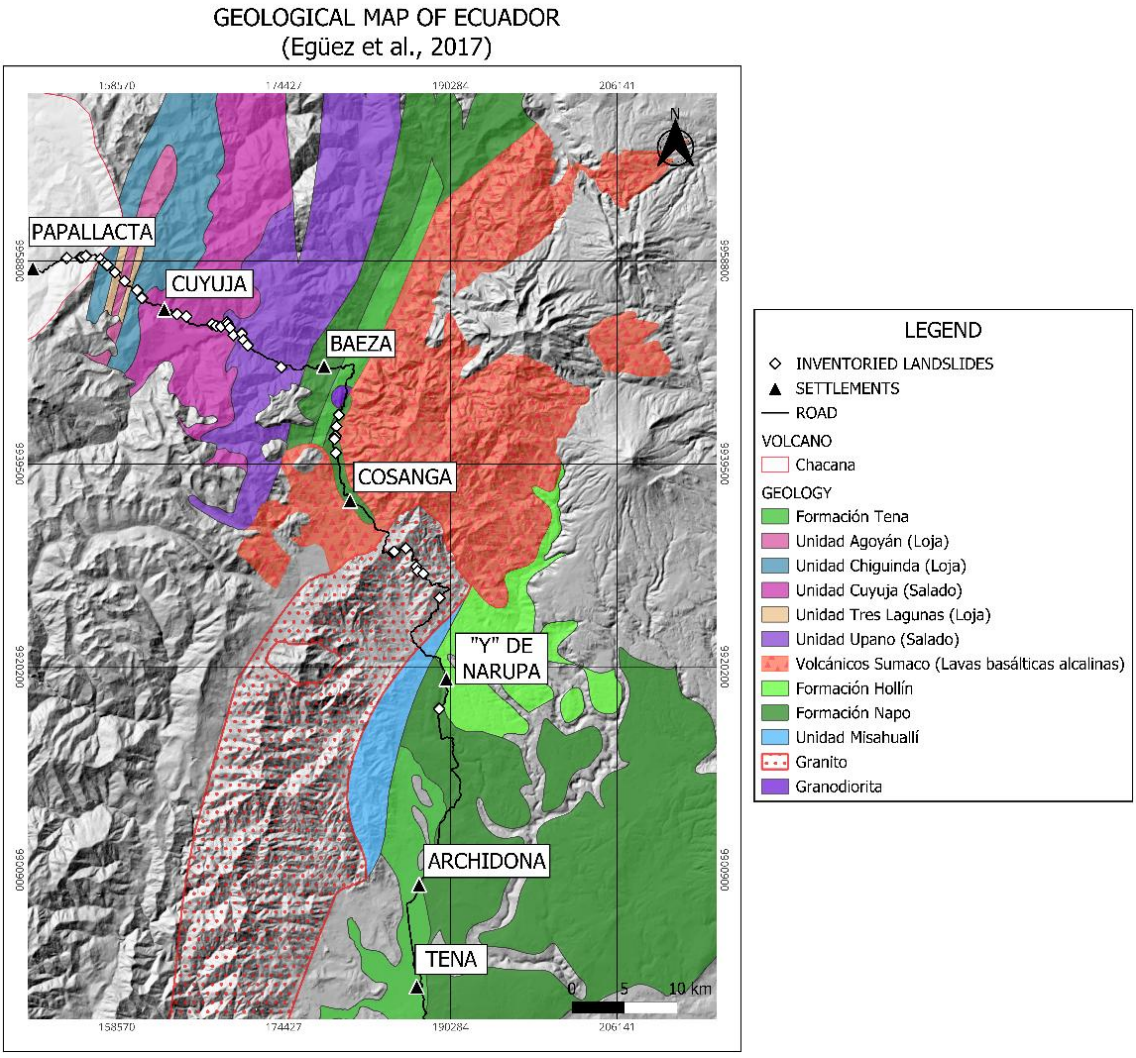

Figure 2. Geological map of Ecuador based on Égüez et al. (2017), showing only the geological formations through which the road crosses. In addition, the locations of landslides inventoried by Espín et al. (2018) are shown.

2 Methods

This study employed the Mora-Varshson method (1991, 1994), a model developed to assess landslide susceptibility in seismically active tropical regions. The model utilizes five input variables, combining morphodynamic (passive) and triggering (active) factors to identify landslide-prone areas. Passive factors, such as lithology, relative relief, and soil moisture content or mean monthly precipitation, are those that condition slope stability. Triggering factors, including seismicity and intense rainfall, disrupt the equilibrium of slope materials and accelerate mass movement processes.

Each factor is assigned an influence index for a given location. These indices are then combined through multiplication and summation (Eq. 1) to calculate the susceptibility degree (H) (Mora and Varshson, 1994).

$$H = (Sr\ x\ Sl\ x\ Sh)\ x\ (Ts + Tp) \quad (1)$$

Where:

Table 1. Landslide Susceptibility Variables.

Variables	Symbol
Relative relief	Sr
Lithology	Sl
Average monthly humidity or precipitation	Sh
Seismic intensity	Ts
Rainfall intensity	Tp

Source: (Mora and Varhson, 1994)

Landslide susceptibility mapping was conducted using ArcMap as the primary geospatial data processing tool. A raster-based Digital Elevation Model (DEM) was utilized for terrain analysis, and precipitation intensity layers were generated using the Spatial Analyst Tools. The Raster Calculator tool was employed for the final susceptibility calculation.

To validate the susceptibility model, an inventory comprising 38 landslide events, compiled by Espín et al. (2018), was incorporated. This inventory led to a press report published in the newspaper La Hora (2018). This approach facilitated the assessment of the model's accuracy in identifying areas prone to landslides. All layers generated during processing were save in IMG format for subsequent analysis.

2.1 Passive factors

2.1.1 Relative relief (Sr)

This refers to the difference in elevation between the highest and lowest points within a specific area, as expressed in Eq. (2) (Mora and Varshson, 1994).

$$Rr = \frac{h_{max} - h_{min}}{km^2} \quad (2)$$

The relative relief map was generated using vertical dissection (Dv), a parameter that reflects the variation in terrain elevation within a specific area (Priego et al., 2011). To better understand the Dv in the study area, a preliminary field reconnaissance was conducted. This allowed for direct observation of the landscape and identification of zones with greater or lesser elevation variation.

A Digital Elevation Model (DEM) derived from ALOS PALSAR radar data, available from the EARTHDATA database, was used. For the relief analysis, a 300 x 300 meter grid was created using the Data Management Tools > Sampling and Create Fishnet tools in ArcToolbox. This cell size allows for differentiation between maximum and minimum elevations within each cell, which is essential for generating the relative relief map.

To extract the statistics from the grid generated within the DEM, the Spatial Analyst Tools > Zonal > Zonal Statistics as Table tool was employed. This process produced an attribute table displaying the maximum elevation (hmax), minimum elevation (hmin),

and range for each cell. The range, representing the elevation difference within each cell, was used to classify the relative relief.

To perform the interpolation required for generating the Dv map, central points were created from the grid using the Data Management Tools > Features > Feature To Point tool. The resulting points retained all statistical data from the grid, allowing the assignment of X and Y coordinates to each point. Interpolation was performed based on the range values using the Kriging method, which is accessible within the Spatial Analyst Tools suite.

The results of the interpolation were classified using the "Morphometric Classification according to Vertical Dissection (Dv) in m/km2" (Table 2). This classification scheme, adapted from Priego et al. (2011), allows for the categorization of the Dv values into thirteen classes, resulting in the final Dv map.

Table 2. Morphometric classification

Morphometric classification according to vertical dissection (Dv) in m/km²	
Scale 1:250 000 (simple, in 5 classes)	Scale ≥ 1:50 000 (broken down into 3 levels of Dv).
Subhorizontal plains (Dv ≤ 2.5) (without decomposition into degrees of Dv)	
Undulating plains	Slightly dissected (2.6 < Dv < 5)
	Moderately dissected (6 < Dv < 10)
(2.6<Dv<15)	Strongly dissected (11 < Dv < 15)
Acolinate plains	Slightly dissected (16 < Dv < 20)
	Moderately dissected (21 < Dv < 30)
(16<Dv<40)	Strongly dissected (31 < Dv < 40)
Lomerios	Slightly dissected (41 < Dv < 60)
	Moderately dissected (61 < Dv < 80)
(41<Dv<100)	Strongly dissected (81 < Dv < 100)
Mountains	Slightly dissected (101 < Dv < 250)
	Moderately dissected (251 < Dv < 500)
(Dv ≥ 101)	Strongly dissected (Dv ≥ 501)

Source: (Priego et al., 2011)

Once the Dv map was generated, it was reclassified using the Spatial Analyst Tools > Reclass > Reclassify tool. During this process, the minimum and maximum values observed in the statistical analysis were verified to ensure they fell within the range established in Table 2. Subsequently, the map was classified into 11 classes, and in the Break Values section, default values were replaced with those specified in Table 2 to ensure greater accuracy in differentiating between plains and mountainous areas. Following this adjustment, the map was further reclassified into five classes, resulting in the relative relief (Sr) map represented in five categories: very low, low, medium, high, and very high.

2.1.2 Lithology (Sl)

Lithology plays a fundamental role in landslide susceptibility, as the physical and mechanical properties of rocks and soils determine their behavior in response to erosion and mass movements (Bobrowsky, 2013; Guerra et al., 2015; Wieczorek & Snyder, 2009). Geotechnical data is ideal for this evaluation, but in its absence, general geological descriptions of the region can be used. The lithological susceptibility classification (Table 3), adapted from Mora and Varshson (1994), is based on the material type and its observed susceptibility to landslides in the study area, as indicated by the geological map (Egüez et al., 2017). For this reason, the study relied solely on the information available in the geological map of Ecuador. From this map, the different lithologies present in the study area were identified, and their behavior in relation to previously recorded landslides was analyzed.

Table 3. Classification of different lithologies and their susceptibilities.

Lithology	Qualification	Factor Sl
Permeable compact alluvium; permeable limestone, slightly fissured intrusions, basalt, ignimbrite, gneiss, hornfels; low degree of weathering, low water table, clean-rugose fractures, high shear resistance.	Low	1
Higher degree of weathering of above mentioned lithologies and of hard massive sedimentary rocks; lower shear resistance and shearable fractures.	Moderate	2
Considerably weathered sedimentary, intrusive, metamorphic, volcanic rocks, compacted sandy regolithic soils, considerable fracturing, fluctuating water tables.	Medium	3
Considerably weathered, hydrothermally altered rocks of any kind, strongly fractured and fissured, clay-filled; poorly compacted pyroclastic and fluvio-lacustrine soils, shallow water tables.	High	4
Extremely altered rocks, low shear resistant alluvial, colluvial and residual soils, shallow water tables.	Very high	5

Source: (Mora and Varhson 1994)

Geological formations, determined by their lithology, degree of consolidation, and permeability, are among the key factors influencing landslide susceptibility (Althuwaynee and Pradhan, 2017; Salehpour Jam et al., 2021).

The lithology map (Sl) was developed based on geological information from the "Geological Map of the Republic of Ecuador" (Egüez et al., 2017), which was digitized into a shapefile (shp) format. The geological formations in the study area comprise diverse rock types, including sedimentary, metamorphic, volcanic, and intrusive formations. The Napo, Tena, and Hollín formations are prominent sedimentary units.The Upano, Cuyuja, and Chiguinda units, along with the Abitagua granite intrusion,

also represent significant geological features in the study area. Additionally, Quaternary volcanic deposits from Sumaco Volcano contribute to the region's geological complexity.

Lithological susceptibility (Sl) was assigned to each geological unit based on the classification in Table 3, considering the material type and its predisposition to landslides. To reflect the spatial variability of susceptibility within a given unit, the Cut Polygons tool was used to subdivide lithological units into different polygons. For example, the Napo Formation was divided into two polygons, assigning a differentiated Sl value to the area where it outcrops at the surface and landslides have been recorded, compared to the area where it does not outcrop. This differentiation is essential, as geological formations can exhibit varying degrees of susceptibility to landslides depending on their degree of exposure to surface processes. Outcropping lithologies are directly subjected to weathering, erosion, and fracturing, which reduce their mechanical strength and increase their susceptibility to failure. In contrast, the same lithology at greater depths may remain more intact, preserving its original geomechanical properties and thus exhibiting lower susceptibility to landslides (Domínguez & Álvarez, 2018).

This phenomenon has been documented in multiple studies. For instance, research conducted in the Baracoa-Cajobabo sector, Cuba, identified significant variations in landslide susceptibility within the same geological formation. Areas where rock units were exposed to surface conditions displayed increased weathering, greater fracturing, and consequently higher landslide occurrence compared to non-outcropping sections (Domínguez & Álvarez, 2018). Similarly, an analysis of the Alóag-Santo Domingo road corridor in Ecuador highlighted the role of lithological exposure in slope stability, where surface-exposed rock masses demonstrated reduced cohesion and strength, leading to increased susceptibility (Orejuela, 2020).

To generate the lithological susceptibility (Sl) map in raster format, the Conversion Tools > To Raster > Polygon to Raster tool was used. The "CLASS" column of the lithological units shapefile was utilized to assign susceptibility values to each raster cell. The

resulting SI map is represented in five susceptibility classes: very low, low, moderate, high, and very high, and will be employed as a variable in the susceptibility equation (H).

2.1.3 Soil Moisture (Sh)

The most accurate method for determining soil moisture is through direct field measurements. However, resource limitations cannot be applied on a large scale, as in the present study. Mora and Varhson (1991) propose a simplified approach where only the average monthly precipitation is used as an input parameter.

To this end, mean monthly precipitation records were categorized into three distinct ranges to facilitate their use in subsequent analysis (Table 4). These ranges vary from 0 to 2, where values below 125 mm/month are assigned a value of 0, and values greater than or equal to 250 mm/month are assigned a value of 2 (Mora and Varshson, 1994).

Table 4. Classification of average monthly values of rainfall.

Average Monthly Precipitation (mm/month)	Assigned Value
<125	0
125-250	1
>250	2

Source: (Mora and Varhson, 1994)

Raster data for developing the soil moisture (Sh) map was obtained from the National Institute of Meteorology and Hydrology (INAMHI, 2024). This dataset contains information on mean monthly precipitation from 1985 to 2015, including maximum and minimum precipitation averages for each month, as well as an annual value.

The Raster Calculator tool was used to calculate the mean monthly precipitation by summing the precipitation values for all months and dividing the result by 12. Subsequently, the relevant portion of information for the study area was extracted using the Extract by Mask tool (Spatial Analyst Tools > Extraction).

Based on Table 4, which classifies mean monthly precipitation values, the maximum value (2) was assigned to the study area using the Reclassify tool (Spatial Analyst Tools > Reclass). This reflects the high average annual precipitation historically recorded in the study area.

2.2 Triggering Factors

2.2.1 Seismicity (Ts)

The seismic zonation map of Ecuador, established in the Ecuadorian Construction Code (NEC), divides the territory into six seismic zones, each with a specific seismic acceleration expressed as a fraction of gravity (g). These values represent the horizontal force that infrastructures must withstand to minimize damage during seismic events, making them a fundamental parameter in the design and construction of roads, bridges, buildings, and housing to ensure structural stability and safety. In this study, the seismic zonation map based on NEC-11 (2015) was used and adapted into a shapefile (shp) format for geospatial analysis. Special emphasis was placed on seismic zones 4 and 5, which exhibit high and very high seismic accelerations, where our study area is located.

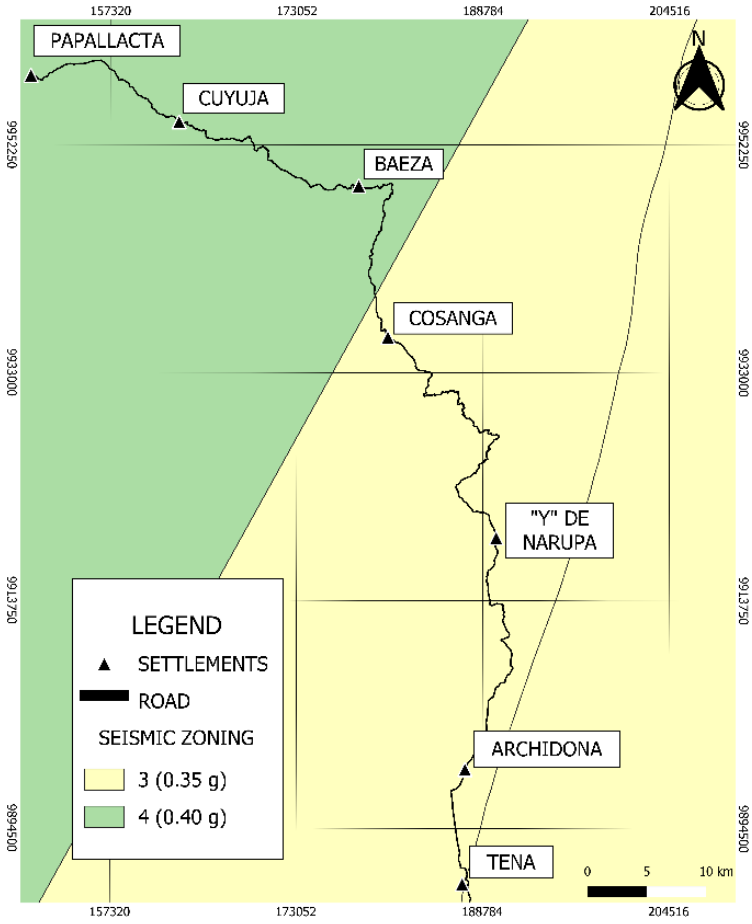

Figure 3. Shows the seismic zonation map of Ecuador, which defines different seismic zones based on ground acceleration values, as established in the Normativa Ecuatoriana de la Construcción NEC-11 (2015).

To generate the seismic intensity map (Ts), the seismic zonation map of Ecuador (Figure 3), which represents the expected seismic acceleration in different regions of the country, was used as a base.

First, the seismic zonation map was converted from vector (polygon) format to raster format using the Conversion Tools > To Raster > Polygon to Raster tool. The attribute data representing the seismic acceleration values was used as the basis for the conversion. Thus, obtaining the variable seismicity map.

2.2.2 Precipitation intensity (Tp)

The occurrence of landslides in tropical regions is significantly influenced by high-intensity rainfall, which is considered the second most important triggering factor (Mora and Varshson, 1991).

Calculating rainfall intensity (Tp) with return periods of 100 years or less is crucial in assessing landslide susceptibility, particularly when applying the methodology proposed by Mora and Varshson (1994). To determine the Tp value, records of maximum rainfall within a 24-hour period were utilized.

Recent studies emphasize the importance of considering extreme rainfall events in landslide susceptibility assessments. Mtibaa and Tsunetaka (2023) found that the highest landslide densities occurred in areas where precipitation exceeded return periods of 100 years at multiple time intervals (from 1 to 72 hours). This suggests that although such events are rare, they represent critical conditions for slope instability. Additionally, failing to incorporate longer return periods—such as 100 years or more—could lead to an underestimation of landslide susceptibility, as shorter return periods (e.g., 10 or 25 years) may not adequately capture the most extreme rainfall events that drive mass movements (Mtibaa & Tsunetaka, 2023).

The construction of the rainfall intensity map was based on data extracted from meteorological yearbooks published by the National Institute of Meteorology and Hydrology (INAMHI, 2024), covering the period from 1971 to 2013. To determine the Tp value, records of maximum rainfall within a 24-hour period were utilized.This time range was selected due to the absence of more recent publications from the institution responsible, which has not provided information for the last 12 years, at least not on its official website. The first step involved identifying meteorological stations near the study area (see Table 5).

Table 5. Meteorological Stations

Stations	Own identification code	X	Y	Zone
Papallacta	E1	817847.00	9959606.00	WGS 84 / UTM zone 17S
Tena	E2	186803.80	9891026.20	WGS 84 / UTM zone 18S
Borja Quijos	E3	185466.30	9953981.60	WGS 84 / UTM zone 18S
El Chaco	E4	188960.10	9963819.50	WGS 84 / UTM zone 18S
Archidona	E5	184230.70	9896926.30	WGS 84 / UTM zone 18S
Zatzayacu	E6	182029.30	9868150.60	WGS 84 / UTM zone 18S
Sardinas	E7	188126.00	9958931.60	WGS 84 / UTM zone 18S
Cotundo	E8	184132.80	9903351.10	WGS 84 / UTM zone 18S
Chonta Punta	E9	238464.50	9896751.10	WGS 84 / UTM zone 18S
Baeza	E10	180980.80	9949153.60	WGS 84 / UTM zone 18S

Source: INAMHI (Meteorological Yearbooks)

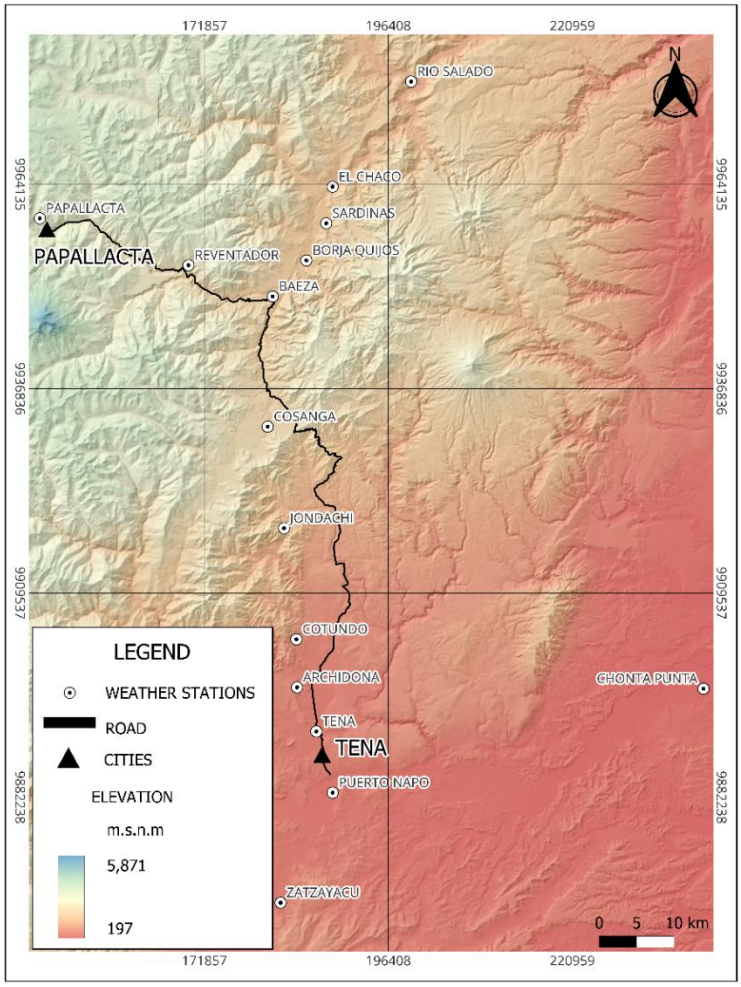

Figure 4. Map of the location of the meteorological stations used for the calculation of precipitation intensity.

After identifying the meteorological stations, Pmax (maximum precipitation) data recorded in each meteorological yearbook over a 42-year period were extracted (see Table 6). As some stations exhibited gaps in their records over extended periods, and adhering to the recommendations of Mora and Varshson (1991, 1994) to analyze time series of at least ten years, priority was given to obtaining a minimum of eight Pmax records per station. This approach ensures statistical representativeness and temporal continuity of the data, guaranteeing that the selected values accurately reflect the maximum precipitation conditions during the study period.

Table 6. Pmax values in mm/day recorded from 1971 to 2013 at the meteorological stations.

Own identification code: Meteorological Stations

N° Pmax recorded	E1	E2	E3	E4	E5	E6	E7	E8
1	100	119	150.4	41.5	103.2	117	46	157.8
2	91.7	100.6	75	69.8	90.4	141.1	104.2	85.9
3	56.8	106.5	60	69.4	82.6	128.8	32	119.6
4	70.6	102.6	66	69.8	80.4	175.3	198	78.3
5	30.8	110.3	66.4	78.5	70	54.3	54.7	16
6	67.2	110.4	74.3	74	90.3	44.7	54	84.9
7	44	92.2	105	57.7	107.7	77.6	52.4	69.4
8	73.8	82	191	60.7	86.4	95.6	40.9	100
9	45	147.1	100	60.9	83.5	83.8	96	95
10	31.9	110.5	95.1	50.7	137.3	85.2	63.3	70.8
11	68.2	98	60.6	50.5	146	119.2	63.3	80
12	47.6	90.7	68.1	79.5	89.1	87	65.6	69.3
13	54.7	81.7	52.3	58.7	132.3	203	64.7	71.7
14	37.2	96.4	124.5	78	107.1	73.5	101.6	
15	48.7	130.5	45.2	62.6	85.3	163.4	165	
16	43.3	126.4	32	45.3	141.7	254.2		
17	54.1	90.6	34.8	51.2				
18	36.5	147.2	80.9					
19	38.5	110.6	63.7					
20	183	223						
21	54.5	175.3						
22	52.2	104.5						
23	30.5	125.9						
24	43							
25	26							

26	65.2							
27	50							
28	32							
29	35.2							

	Own identification code: Meteorological Stations							
N° Pmax recorded	**E9**	**E10**	**E11**	**E12**	**E13**	**E14**	**E15**	**E16**
1	108.1	62.4	73	99.1	171	97.1	102.2	121.4
2	116.3	43.6	59	102	86.1	95.8	90.5	130
3	145.5	47.9	55.2	113.5	75.7	97.9	64.4	114.3
4	104.7	61.2	74.6	94.2	169.7	84.5	71	119.4
5	132.9	56.5	87.2	92.8	108.8	113.8	57.2	103.4
6	110.6	83	52.7	141.9	161.6	73.3	65.5	140.7
7	109.8	80	55.4	89.4	150.8	115.9	63.2	127.4
8	157	70.3	61.2	102.2	140	116.9	90.3	106.3
9	99.9	66.2	80	98	81	129.9	54	
10	86.7	70.7	79.4	85	110.5			
11	126.3							
12	141.2							
13	96.7							

Source: (INAMHI) (Meteorological Yearbooks)

To estimate the precipitation intensity associated with a 100-year return period, the HIDROESTA 2 software (Villón, 2014) was used. This program implements the Gumbel distribution, a methodology recommended by Mora and Varhson (1994) for the analysis of extreme events. The Gumbel distribution is widely used in the modeling of extreme hydrometeorological events, as it allows robust and reliable estimates of precipitation intensity, with a confidence level of 95 % ($\alpha = 0.05$) (Sasireka et al., 2019). The process begins by loading an Excel spreadsheet containing the maximum precipitation (Pmax) data for each meteorological station, which allows for specific calculations for each

location. Given that the available time series spans 42 years, it is necessary to extrapolate the maximum precipitation values corresponding to a 100-year return period, considering a 24-hour duration.

The process continued with importing the data into ArcMap using comma-delimited files. Spatial interpolation, using Inverse Distance Weighting (IDW), was then applied to estimate values in areas lacking data (Choi & Chong, 2022). Additionally, according to Andrade & Moreano (2013), IDW generated better results for precipitation in Ecuador when considering a wider altitudinal range, making it suitable for the study area, which has a significant altitudinal gradient. They demonstrated that IDW presented the lowest errors for the precipitation variable compared to Kriging and Modified Shepard interpolation methods. This function is available in Spatial Analyst Tools > Interpolation. After obtaining the interpolation results, the data was reclassified using the Spatial Analyst Tools > Reclass > Reclassify tool, based on the criteria presented in Table 7, which details the classification of maximum daily rainfall for different return periods.

Table 7. Rainfall intensity factor (Tp) resulting from the classification of maximum daily rainfall for a return period of 100 years and 10 years or less.

Maximum Rainfall (n > 10 yr; Tr = 100 yr)	**Rainfall (n < 10 yr; Average)**	**Qualification**	**Factor Tp**
< 100 mm	< 50 mm	Very low	1
101–200 mm	51–90 mm	Low	2
201–300 mm	91–130 mm	Medium	3
301–400 mm	131–175 mm	High	4
> 400 mm	> 175 mm	Very High	5

Source: (Mora and Varhson, 1994)

After generating individual maps for each variable of the susceptibility model, they were integrated using Eq. (1) in the Raster Calculator (Spatial Analyst Tools > Map Algebra). This process generated a preliminary landslide susceptibility map.

Subsequently, the preliminary map was reclassified into five susceptibility classes (Very Low, Low, Moderate, High, and Very High) using the Reclassify tool (Spatial Analyst Tools > Reclass). The final output is a landslide susceptibility map categorized into these five classes.

3 Results and Discussions

3.1 Passive factors

3.1.1 Relative relief (Sr)

Morphometric analysis, based on vertical dissection (Dv) and expressed in m/km², reveals significant topographic heterogeneity within the study area (Figure 5A). Values range from plains (Level 1: 7.055-52.140 m/km²) to severely dissected mountainous terrain (Level 11: 668.296-965.102 m/km²). The use of a high-resolution DEM derived from ALOS PALSAR radar data allowed a more accurate capture of topographic variations, resulting in higher Dv values.

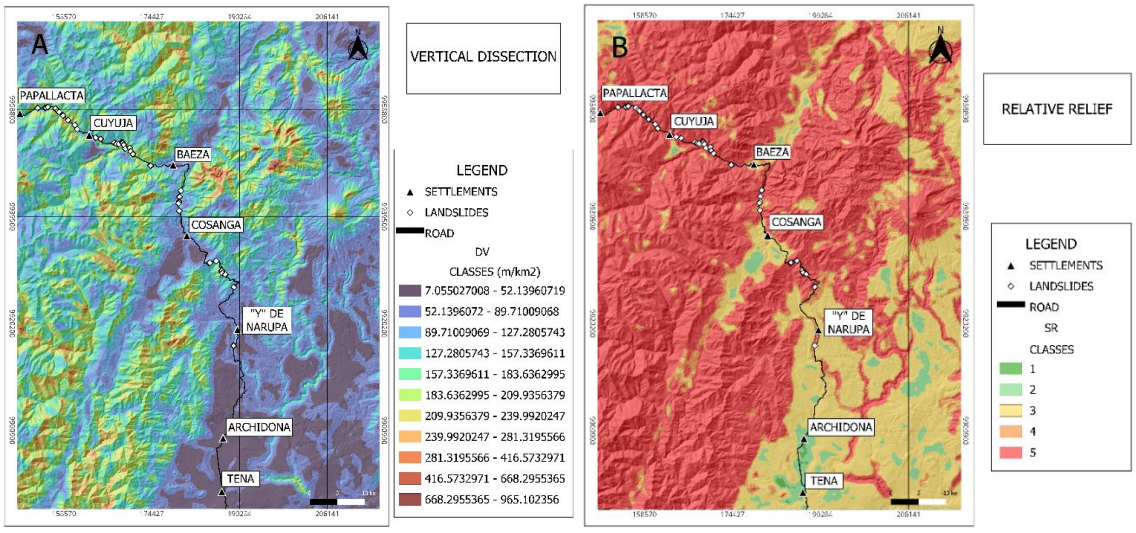

Figure 5. Relative Relief Maps for the Tena-Papallacta Road. (A) Vertical dissection (Dv) classified into 11 levels. (B) Relative relief (Sr) classified according to the Mora-Varshson methodology.

The distribution of Dv levels shows a gradual transition from areas of low dissection, such as plains and gentle slopes (Levels 1-3), towards mountainous zones with increasing vertical dissection (Levels 4-11). This trend aligns with the geological and tectonic setting of the region, characterized by the presence of active faults and orogenic uplift processes that generate rugged topography (Alvarado et al., 2014). Levels 4-6 mark the transition to more rugged terrain, with steeper slopes and a higher incidence of geomorphological features such as hills and ridges. Levels 7-11 characterize

mountainous regions with abrupt topography, culminating in areas with pronounced elevation differences.

The range of relative relief (Sr) spans from sub-horizontal plains (Very Low Relief) with vertical dissection (Dv) between 7.055 and 52.140 m/km² to highly fragmented mountainous terrain (Very High Relief) with Dv exceeding 281.320 m/km². The Dv values quantify this heterogeneity, exhibiting high values in mountainous areas, which suggests greater susceptibility to landslides due to the presence of steep slopes and unstable hillslopes (Nguyen et al., 2020). In contrast, areas with low Dv, corresponding to plains and valleys, exhibit lower susceptibility.

Analysis of the Sr, derived from the Dv map, complements the understanding of landslide susceptibility. Areas with higher Sr (high and very high) coincide with zones of high Dv, further confirming the direct relationship between these two parameters (Mora & Varshson, 1994). These areas, characterized by steep slopes and abrupt elevation changes, are prone to landslides, especially in the presence of triggering factors such as intense rainfall or earthquakes (Barrantes Castillo et al., 2011).
While the Dv results differ from the ranges proposed by Priego et al. (2011), this discrepancy underscores the importance of considering the specific geomorphological characteristics and data resolution of the study area. Adapting the classification of Priego et al. (2011) to the local topographic reality allowed for a more accurate representation of Dv and its influence on relative relief.

3.1.2 Lithology (Sl)

The analysis identified 24 distinct lithological units, distributed across 120 polygons, with susceptibilities ranging from very low (Sl 1) to very high (Sl 5) (Figure 6). The classification was based on lithological composition, the presence of historical landslides, and the criteria outlined in Table 3. Areas with higher susceptibility (Sl 3-5) are concentrated in the mountainous zone's northwest of the road, between Papallacta and Baeza.

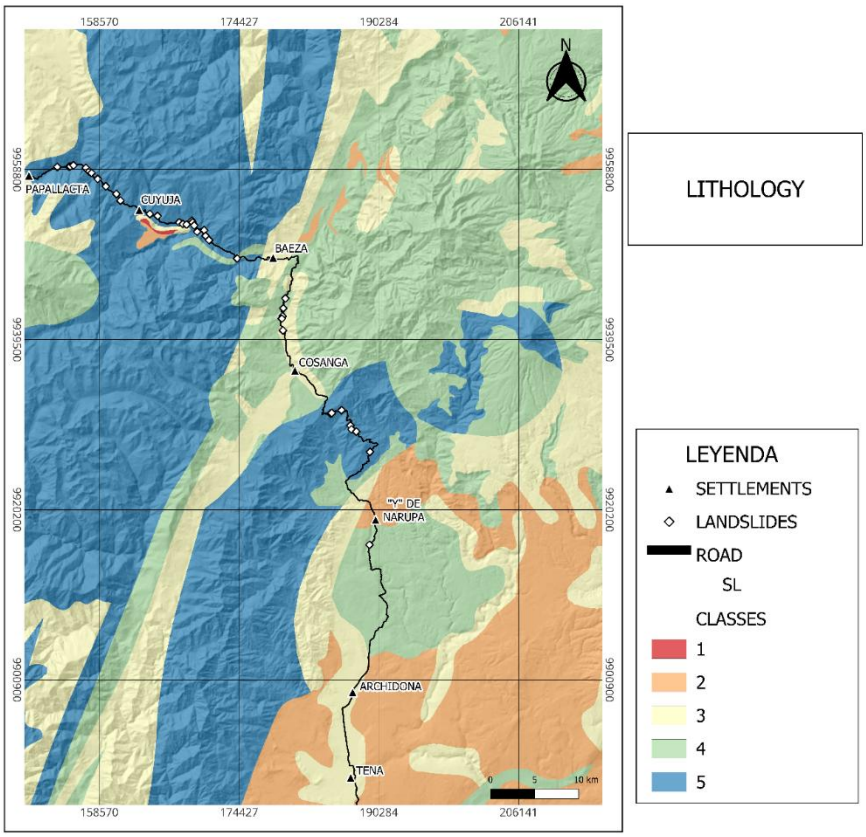

Figure 6. Lithology map (Sl) for the Tena-Papallacta road, classified according to the Mora-Varshson methodology.

Zones with Sl 1-2, predominantly composed of consolidated lithologies such as whose materials are composed primarily of shales and limestones, exhibit distinctive characteristics. These include a low degree of weathering, a reduced or absent water table, clean and rough fractures, and high shear strength. These factors limit the development of failure surfaces and, consequently, decrease the likelihood of mass movements (Zhang et al., 2023; Wyllie & Mah, 2004; Hencher, 2004). As a result, these zones display low susceptibility to landslides.

Conversely, areas with Sl 3-5, dominated by more susceptible lithologies such as highly weathered rocks, residual soils, and poorly consolidated deposits, exhibit moderate to very high susceptibility to instability processes. Weathering, both physical and chemical, significantly weakens the cohesion of the rock matrix, decreases its mechanical strength, and increases porosity, promoting water infiltration and the consequent increase in pore water pressure (Selby, 1993).

Within the Napo Formation, surface outcrops, which are more exposed to weathering and show evidence of historical landslides, exhibit a higher SI than areas where the formation is located at depth.

3.1.3 Soil Moisture (Sh)

Analysis of the mean monthly precipitation (Sh) in the study area, derived from historical data between 1985 and 2015, revealed a predominance of high precipitation values, categorized as 2 according to the methodology of Mora and Varshson (1994). This indicates that the mean monthly precipitation exceeding 250 mm.

.

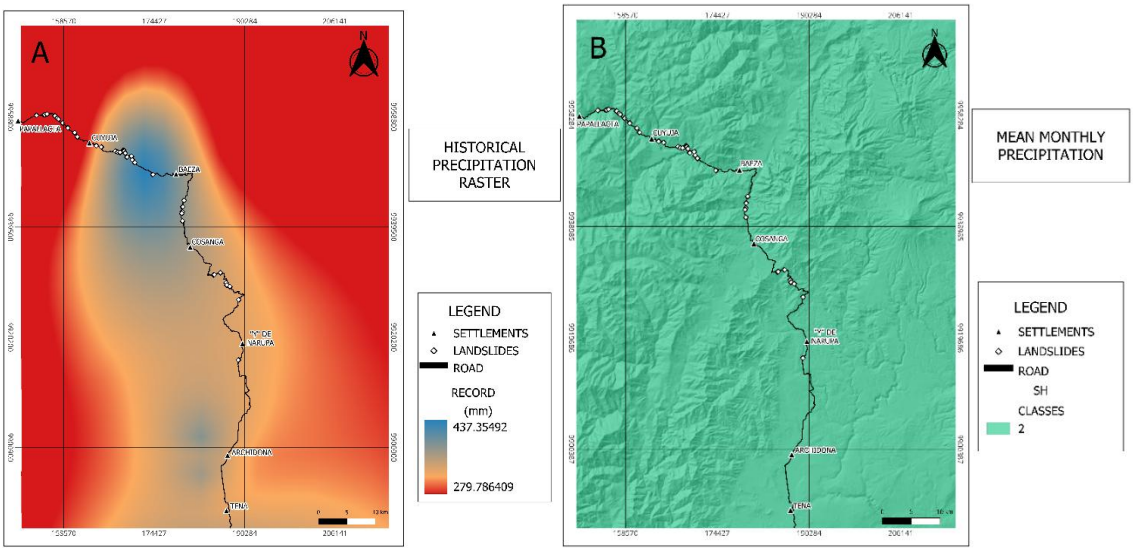

Figure 7. Precipitation maps for the Tena-Papallacta road. (A) Historical precipitation record (1985–2015) in raster format. (B) Mean monthly precipitation map (Sh) classified according to the Mora–Varshson methodology.

While the analysis of the precipitation time series data shows that August has the lowest monthly average (with a maximum record of 371 mm) and April the highest (with a maximum record of 731 mm), it is crucial to highlight that all months of the year exceed the 250 mm/month threshold established for category 2 in Table 4. This signifies that, on average, monthly precipitation in the study area consistently surpasses 250 mm, justifying the assignment of class 2 in the mean monthly precipitation map.

The high precipitation recorded in the study area, attributable to its geographic location and the influence of the Intertropical Convergence Zone (ITCZ) (Byrne et al., 2018), constitutes a significant conditioning factor for landslide occurrence. The ITCZ, a region of low atmospheric pressure where trade winds from the Northern and Southern Hemispheres converge, generates a band of clouds and storms that produce intense rainfall in equatorial regions (Insel et al., 2010; Byrne et al., 2018; Espinoza et al., 2020). Furthermore, the presence of the Andes Mountains acts as an orographic barrier, intensifying precipitation on the eastern slopes where the study area is located (Garreaud, 2009; Insel et al., 2010; Espinoza et al., 2020).

Soil saturation, resulting from high precipitation, decreases shear strength, reduces cohesion between soil particles, and increases pore pressure, thereby enhancing the likelihood of mass movements (Nguyen et al., 2020; Yin et al., 2023). In rocky materials, saturation also plays a significant role, although the mechanism differs. Water infiltrating rocks can cause the expansion of existing cracks, the reduction of internal strength, and the generation of chemical weathering processes that weaken their structure, increasing their susceptibility to failure (Oyanguren & Monge, 2004).

This effect of saturation, in both soils and rocks, is exacerbated in areas with steep slopes, such as those found in the study area. The combination of high slopes and saturated materials creates conditions highly conducive to landslide occurrence. Therefore, it is crucial to consider both soil properties and rock characteristics when assessing landslide susceptibility in geologically complex regions.

3.2 Triggering Factors

3.2.1 Seismicity (Ts)

The seismic acceleration map (Ts) generated for the Tena-Papallacta road (Figure 8) demonstrates a clear influence of seismic activity on landslide susceptibility in the study area. The analyzed segment is located within seismic zone 4 and 5 of the Ecuadorian seismic zonation (NEC-11, 2015), characterized by a seismic acceleration of 0.35 g to

0.40 g, according to NEC, (2015). This zone exhibits considerable potential for the generation of seismically induced landslides.

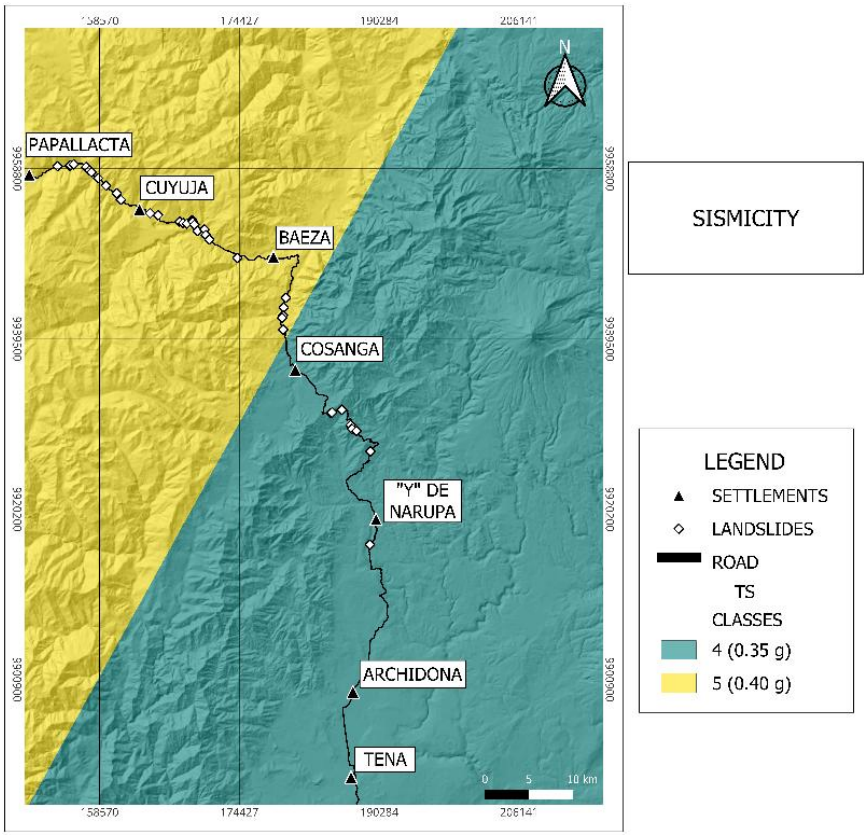

Figure 8. Ground acceleration map (Ts) for the Tena-Papallacta road, showing the classification in relation to influence.

Seismicity in the region results from the complex interaction of several geodynamic processes, including the subduction of the Nazca Plate beneath the South American Plate, the activity of the dextral-reverse transcurrent system of the Inter-Andean Valley and Northeast, and the presence of reverse faults in the Sub-Andean front (Alvarado et al., 2014; Quilumba, D., 2021).

The obtained Ts values, ranging from 4 to 5, indicate a very high susceptibility to seismically induced landslides. These values, based on the Mora-Varshson model (1994), suggest that seismic intensity in the area is a key factor determining slope stability, especially in areas with higher Ts values where the majority of landslides are concentrated. This is because seismicity acts as a trigger, destabilizing slopes and causing

mass movements, particularly in areas with steep gradients and susceptible geological materials (Mora and Varshson, 1994).

3.2.2 Precipitation intensity (Tp)

Assessing landslide susceptibility requires analyzing rainfall intensity due to its role as a triggering factor in tropical regions (Mora and Varshson, 1991). In this study, rainfall intensity for a 100-year return period was calculated using 24-hour maximum precipitation (Pmax) data from meteorological stations near the study area (INAMHI, 2024.). Table 8 presents the results obtained using the HIDROESTA 2 software (Villón, 2014).

Table 8. Calculation of the 100-year return period rainfall intensity in mm/day.

Stations	PR_10	PR_100
Papallacta	94.3	149.33
Tena	158.77	217.98
Borja Quijos	133.17	205.98
El Chaco	77.79	99.58
Archidona	133.87	178.51
Zatzayacu	193.17	297.36
Sardinas	141.03	216.04
Cotundo	126.65	185.83
Chonta Punta	145.46	183.84
Baeza	80.73	103.97
Cosanga	84.01	106.82
Jondachi	122.85	152.40
Reventador	174.51	243.32
San Rafael-Napo	126.02	158.64
Río Salado	95.26	126.32
Puerto Napo	136.57	159.33

The meteorological stations exhibit considerable variability in rainfall intensity for both return periods. This can be attributed to factors such as topography, altitude, and the influence of the Andes Mountains on precipitation patterns (Insel et al., 2010; Garreaud, 2009).

It is important to emphasize that the rainfall intensity for a 100-year return period is significantly greater than that for a 10-year return period across all stations. This highlights the importance of considering low-probability, extreme events in landslide susceptibility assessments, as these events can generate disproportionate impacts on terrain stability (Nguyen et al., 2020).

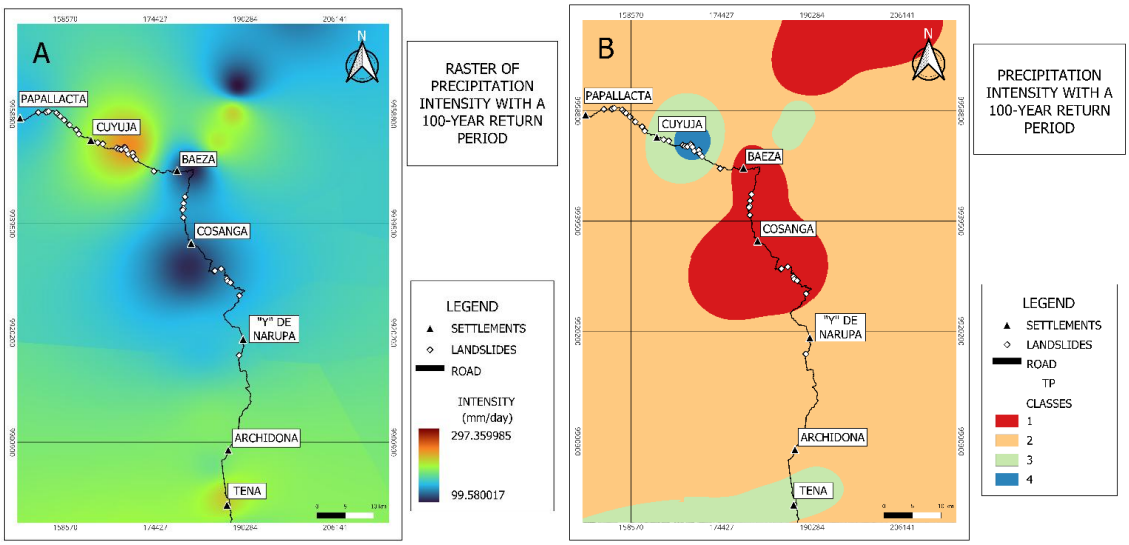

Figure 9. Precipitation intensity maps for the Tena-Papallacta road. (A) Rainfall intensity with a 100-year return period, obtained through IDW interpolation. (B) Rainfall intensity map (Tp) classified according to the Mora-Varshson methodology.

Analysis of rainfall intensity (Figure 9A) reveals a heterogeneous spatial distribution, with maximum precipitation values concentrated in the mountainous areas to the west. This spatial heterogeneity can be attributed to orographic effects, where the forced ascent of moist air over mountain slopes causes cooling and condensation, generating more intense rainfall at higher elevations (Barry, 2008; Sidle et al., 2006).

Figure 9B shows the classification of rainfall intensity into four categories, with class 4, which has values close to 297.36 mm/day, representing the highest intensity. These maximum intensities are concentrated in the mountainous areas to the west. Although

these values do not reach the 300-400 mm/day threshold proposed by Mora-Varshson (1994) for the "Very High" category, their classification as class 4 reflects a conservative approach, acknowledging the risk of intense rainfall in mountainous regions susceptible to landslides.

Analysis of Figure 9B reveals a discrepancy between rainfall intensity and landslide occurrence in the area highlighted in red. Despite exhibiting low rainfall intensity (Tp: 1), this zone records a considerable number of landslides. This discrepancy can be attributed to the influence of geological materials, which, due to their inherent nature and the effects of weathering, can strongly influence landslide susceptibility, even in areas with lower rainfall intensity.

Analysis of Figure 10 reveals the distinct influence of triggering factors (seismicity and precipitation intensity) on landslide susceptibility. In Figure 10B, which considers only seismicity as an active factor, high susceptibility is observed in the segment between the "Y" de Narupa and Papallacta. However, in Figure 10C, which considers only rainfall intensity, high susceptibility is concentrated in the Baeza-Papallacta segment, with a reduction in the susceptibility index observed in the Baeza-"Y" de Narupa segment.

This difference in the spatial distribution of susceptibility suggests that rainfall intensity plays a significant role in determining susceptibility in the Baeza-"Y" de Narupa segment. The scarcity of meteorological stations (two stations over approximately 48.04 km of road) could influence the accuracy of the rainfall intensity analysis and, consequently, the susceptibility assessment. It is possible that the low density of meteorological stations does not adequately capture the spatial variability of rainfall in this segment, potentially underestimating rainfall intensity in certain areas. Furthermore, the geological and geomorphological characteristics of this section, such as the presence of slopes that channel precipitation, could contribute to the frequency of landslides. The concentration of surface flow, whether by the channeling of precipitation or erosion caused by subsurface flow, intensifies erosive processes and increases slope instability,

thereby raising the probability of landslide occurrence (Lobkovsky et al., 2004; Olarte, 2017).

Figure 10A presents the final susceptibility map obtained by incorporating both triggering factors (seismicity and rainfall intensity). In this map, steep slopes contribute significantly to terrain instability. As previously mentioned, vertical dissection (Dv) reflects the variation in terrain elevation within a specific area. High Dv values indicate the presence of steep slopes and rugged terrain, which increases susceptibility to landslides, especially in the presence of low-strength materials such as weathered rocks or regolithic soils. Moreover, high precipitation, which can exceed 400 mm/month, saturates the soil, increasing the weight of the terrain and reducing the cohesion of materials, further increasing landslide susceptibility. Seismic acceleration, reaches up 0.40 g in the study area, also plays a crucial role in landslide generation. It is important to consider that the combination of an earthquake followed by intense rainfall can significantly increase landslide susceptibility. An example of this occurred in El Salvador in 2001, where an earthquake followed by heavy rains triggered a large number of landslides (Vázquez, 2002).

Studies conducted in other mountainous regions with geological and climatic characteristics similar to those of the study area confirm the importance of the interaction between seismicity and precipitation in landslide generation. López et al. (2020) applied the Mora-Varshson method in a mountainous area of Colombia dominated by sedimentary and metamorphic rocks. The authors found that the interaction between seismicity and rainfall increased landslide susceptibility, particularly on slopes with steep gradients and low-strength materials. These results are consistent with those obtained in the present study, suggesting that the interaction between seismicity and rainfall is a key factor in landslide generation in tropical mountain areas.

It is important to highlight that the landslide inventory compiled by Espín et al. (2018) indicates that the types of mass movement phenomena occurring along the road

corridor include rockfalls, rotational slides, translational slides, creep, and debris flows. Debris flows are the most frequent, representing 50% of the inventoried landslides. In the Baeza-"Y" de Narupa segment, the predominance of debris flows suggests that slopes effectively channel rainfall, leading to concentrated water flow and the entrainment of material at specific points along the road.

This finding underscores the importance of considering the synergistic interaction between passive and triggering factors in landslide susceptibility assessments. Landslide risk management in the area should account for the constant influence of seismicity and the need to implement mitigation measures that reduce slope susceptibility, even in zones with low rainfall intensity.

The presence of landslides in areas of lower susceptibility (Class 3) suggests the influence of additional factors not considered in the model, such as deforestation or other anthropogenic activities. It is important to acknowledge that the susceptibility model used in this study focuses on the interaction of geological, climatic, and seismic factors. Incorporating anthropogenic factors in future studies could enhance the model's accuracy and enable better prediction of landslide occurrences.

Furthermore, the installation of additional rain gauges in the study area could improve the accuracy of precipitation intensity analysis. As mentioned earlier, the scarcity of rain gauges may lead to an underestimation of rainfall intensity in certain areas, which could, in turn, affect the landslide susceptibility assessment. A higher number of stations would allow for a more precise capture of precipitation's spatial variability, particularly in areas with significant topographic variability. This is crucial in mountainous regions such as the study area, where precipitation can vary considerably over short distances. Additionally, the installation of rain gauges would enable the monitoring of soil moisture conditions and the generation of early warnings in the event of heavy rainfall, as landslides have regularly occurred during intense precipitation events. The data obtained from these stations would be invaluable for landslide risk management and the protection of the population.

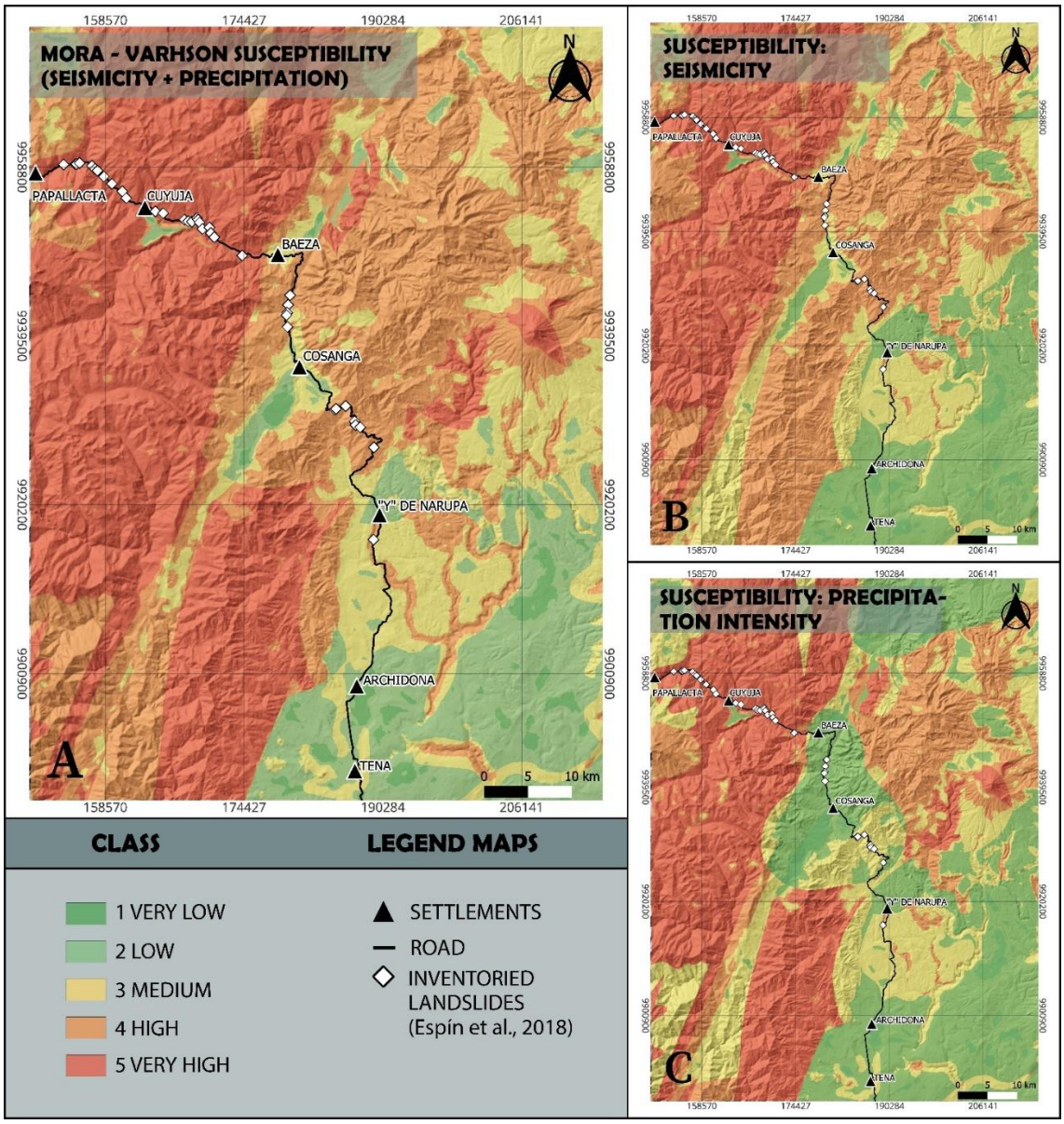

Figure 10. Landslide susceptibility maps for the Tena-Papallacta road. (A) Final susceptibility obtained using the Mora-Varshson method, incorporating both triggering factors (seismicity and precipitation intensity). (B) Susceptibility derived considering only seismicity as a triggering factor. (C) Susceptibility calculated including only precipitation intensity as a triggering factor.

4 Conclusions

The landslide susceptibility analysis revealed that the zone with the highest susceptibility (Class 5) is located in the northwest, specifically between Papallacta and Baeza. From Baeza, through Cosanga to the "Y" de Narupa, the susceptibility index ranges from Class 4 to Class 2 in the central part. Between the "Y" de Narupa and Tena, classes 3 and 2 predominate.

Passive factors, particularly relative relief with pronounced vertical dissection (>101 m/km²) and the presence of weathered and highly fractured geological materials (gneisses, deformed granites, schists, metalavas, metagraywackes, sandstones, limestones, shales, and alkaline basaltic lavas from the Sumaco volcano), have a significant influence on landslide susceptibility. In the presence of rainfall, these conditions facilitate the activation of mass wasting processes.

Validation of the susceptibility model confirms its effectiveness in identifying areas with a high probability of instability. 97.37% of the inventoried landslides fall within zones of very high and high susceptibility (Classes 4 and 5). This information is crucial for risk management and land-use planning in the region, enabling responsible entities, such as the Ministry of Transportation and Public Works (MTOP), to focus on these areas for more detailed studies and the implementation of preventive and corrective measures. The identification of these critical areas will help guide the implementation of targeted mitigation measures.

References

Andrade Chávez, L. S., & Moreano, R. (2013). Sistema de Información para la Interpolación de Datos de Temperatura y Precipitación del Ecuador. Revista Politécnica, 32. Recuperado a partir de https://revistapolitecnica.epn.edu.ec/ojs2/index.php/revista_politecnica2/article/view/52

Alcántara Ayala, I., (2000). Landslides: ¿Deslizamientos o movimientos del terreno? Definición, clasificaciones y terminología. Investigaciones Geográficas (Mx), (41), 7-25.

Althuwaynee, O. F., & Pradhan, B. (2016). Semi-quantitative landslide risk assessment using GIS-based exposure analysis in Kuala Lumpur City. Geomatics, Natural Hazards and Risk, 8(2), 706–732. https://doi.org/10.1080/19475705.2016.1255670

Aristizabal, E., & Hermelin, M. (2011). Propuesta de zonificación del suelo para la gestión del riesgo enfocada al ordenamiento territorial. Gestión y Ambiente, 14(2), 07-16. https://repositorio.unal.edu.co/handle/unal/37521

Barrantes Castillo, G., Barrantes Sotela, O., & Núñez Roman, O. (2011). Efectividad de la metodología Mora-Vahrson modificada en el caso de los deslizamientos provocados por el terremoto de cinchona, Costa Rica. Revista Geográfica de América Central, 2(47), 141-162.

Barrantes, G. (2010). Lecciones aprendidas en gestión de riesgos a deslizamientos: caso zonificación de susceptibilidad por deslizamientos en Cuenca, Ecuador. In I Congreso Internacional Gestión de Riesgos, Ambiente y Energías Alternativas, 10, 11 Y 12 de Noviembre de 2010.

Barry, R. G. (2008). Mountain weather and climate Third edition. https://doi.org/10.1017/cbo9780511754753

Baldock, J. W., Dirección General de Geología y Minas, & Instituto de Ciencias Geológicas. (1982). Geología del Ecuador: Boletín de la explicación del

mapa geológico de la República del Ecuador, escala 1:1,000,000. IGM. https://books.google.com.ec/books?id=EjhCHQAACAAJ

Bobrowsky, P. T. (Ed.). (2013). Encyclopedia of natural hazards. Springer. https://doi.org/10.1007/978-1-4020-4399-4

Brabb, E. E. B. Innovative approaches to landslide hazard and risk mapping: Ponencia de la conferencia. En International Journal Of Rock Mechanics And Mining Sciences & Geomechanics Abstracts 1985, 23-31 de agosto, Japan Landslide Society. https://doi.org/10.1016/0148-9062(87)91363-5

Byrne, M.P., Pendergrass, A.G., Rapp, A.D. et al. Response of the Intertropical Convergence Zone to Climate Change: Location, Width, and Strength. Curr Clim Change Rep 4, 355–370 (2018). https://doi.org/10.1007/s40641-018-0110-5

Choi, K., & Chong, K. (2022). Modified Inverse DistanceWeighting Interpolation for Particulate Matter Estimation and Mapping. ("Spatial Distribution of Particulate Matter (PM2.5) in Klang Valley ...") Atmosphere, 13(5). https://doi.org/10.3390/atmos13050846

Cruden, D. M. (1991). A simple definition of a landslide. Bulletin Of Engineering Geology And The Environment, 43(1), 27-29. https://doi.org/10.1007/bf02590167

Domínguez, S. R., & Álvarez, R. O. (2018). Susceptibilidad por deslizamientos en el sector Baracoa- Cajobabo, provincia Guantánamo, Cuba. GEOS, 38(2).

Egüez, A., Ganoa, M., & Albán, A. (2017). Mapa geológico de la República del Ecuador 2017.

El comercio. (2015). El deslave en la vía a Papallacta afecta incluso a los muertos. El Comercio. Recuperado de 26 de noviembre del 2024, de https://www.elcomercio.com/actualidad/quito/deslave-via-papallacta-afecta-muertos.html

El comercio (2019). Rocas gigantes cayeron sobre un bus interprovincial en la vía Baeza – Tena; hay un fallecido y 13 heridos. El Comercio. Recuperado de 26 de noviembre del 2024, de

https://www.elcomercio.com/actualidad/rocas-deslizamiento-bus-interprovincial-fallecido/

El comercio. (2021). Deslizamiento de tierra en la vía Baeza-Tena dejó un vehículo atrapado; la vía se encuentra habilitada. El Comercio. Recuperado de 26 de noviembre del 2024, de https://www.elcomercio.com/actualidad/ecuador/deslizamiento-tierra-via-baeza-tena-amazonia.html

El universo (2024). Por aluvión en la zona de la vía Papallacta-Baeza se restringió circulación vehicular y tras limpieza se habilitó un carril. Ecuador | Noticias | el Universo. Recuperado de 26 de noviembre del 2024 de https://www.eluniverso.com/noticias/ecuador/quito-papallacta-baeza-circulacion-restringida-nota/

Espín, R., Simbaña, M., & Delgado, C. (2018). Informe técnico sobre los fenómenos de remoción en masa que afectan a la vía, Papallacta - Baeza, Baeza - Cosanga, y Cosanga Tena. Universidad Regional Amazónica IKIAM.

Espinoza, J. C., Garreaud, R., Poveda, G., Arias, P. A., Molina-Carpio, J., Masiokas, M., Viale, M., & Scaff, L. (2020). Hydroclimate of the Andes Part I: Main Climatic Features. Frontiers In Earth Science, 8. https://doi.org/10.3389/feart.2020.00064

Garreaud, R. D. (2009). The Andes climate and weather. Advances In Geosciences, 22, 3-11. https://doi.org/10.5194/adgeo-22-3-2009

Guerra, A. J. T., Fullen, M. A., Jorge, M. C. O., & Bezerra, J. F. R. (2015). Slope processes, mass movements and soil erosion: A review. Journal of Geographical Sciences, 25(5), 603–620. https://doi.org/10.1016/S1002-0160(15)600

Guzzetti, F., Reichenbach, P., Cardinali, M., Galli, M., & Ardizzone, F. (2005). Probabilistic landslide hazard assessment at the basin scale. Geomorphology, 72(1-4), 272-299. https://doi.org/10.1016/j.geomorph.2005.06.002

Hearn, G. J., & Hart, A. B. (2019). Landslide susceptibility mapping: a practitioner's view. Bulletin Of Engineering Geology And The

Environment, 78(8), 5811-5826. https://doi.org/10.1007/s10064-019-01506-1

Hencher, S. R. (2004). Weathering and erosion processes in rock–implications for geotechnical engineering. In Proceedings symposium on Hong Kong soils and rocks (pp. 29-79).

Insel, N., Poulsen, C.J. & Ehlers, T.A. Influence of the Andes Mountains on South American moisture transport, convection, and precipitation. Clim Dyn 35, 1477–1492 (2010). https://doi.org/10.1007/s00382-009-0637-1

Instituto Nacional de Meteorología e Hidrología. (s.f.). Biblioteca. INAMHI. Recuperado 10 de julio de 2024, de https://www.inamhi.gob.ec/biblioteca/

La Hora (2018, 1 mayo). Una megafalla atraviesa la carretera Baeza-Cosanga. Recuperado 21 de febrero de 2025, de https://www.lahora.com.ec/secciones/una-megafalla-atraviesa-la-carretera-baeza-cosanga/

López, R. E., Zuluaga, A. D., Gómez, F., & Tapia, L. (2020). Aplicación del Método Mora-Vahrson para Evaluar la Susceptibilidad a Deslizamiento en el Municipio de Manaure, Cesar, Colombia. Revista de Estudios Latinoamericanos Sobre Reducción del Riesgo de Desastres REDER, 4(2), 57. https://doi.org/10.55467/reder.v4i2.50

Lobkovsky, A. E., Jensen, B., Kudrolli, A., & Rothman, D. H. (2004). Threshold phenomena in erosion driven by subsurface flow. Journal Of Geophysical Research Atmospheres, 109(F4). https://doi.org/10.1029/2004jf000172

Ministerio del Ambiente de Ecuador (2014). Sistema de Clasificación de Ecosistemas del Ecuador Continental. Ministerio del Ambiente de Ecuador.

Mora C. SERGIO, & Vahrson, W. (1994). Macrozonation Methodology for Landslide Hazard Determination. Environmental And Engineering Geoscience, xxxi (1), 49-58. https://doi.org/10.2113/gseegeosci.xxxi.1.49

Mora, S. & Vahrson, W. (1991). Determinación a priori de la amenaza de deslizamientos sobre grandes áreas, utilizando indicadores morfodinámicos. ("(PDF) EFECTIVIDAD DE LA METODOLOGÍA MORA-VAHRSON ... - Academia.edu") En: Memoria sobre el Primer Simposio. Bogotá, Colombia. pp. 259-273.

NEC-11 (2015) Norma Ecuatoriana de la Construcción. Registro Oficial No. 413 del 10 de enero de 2015. Capítulos de la NEC (Norma Ecuatoriana de la Construcción) (Norma Ecuatoriana de la Construcción) (Norma Ecuatoriana de la Construcción) (Norma Ecuatoriana de la Construcción) (Norma Ecuatoriana de la Construcción) (Norma Ecuatoriana de la Construcción) (Norma Ecuatoriana de la Construcción) (Norma Ecuatoriana de la Construcción) – MIDUVI – Ministerio de Desarrollo Urbano y Vivienda (habitatyvivienda.gob.ec).

Nuñez del Arco E., . (2003). Geología del Ecuador. Guayaquil: ESPOL.

Nguyen, B., Lee, S., & Kim, Y. (2020). Spatial probability assessment of landslide considering increases in pore-water pressure during rainfall and earthquakes: Case studies at Atsuma and Mt. Umyeon. CATENA, 187, 104317. https://doi.org/10.1016/j.catena.2019.104317

Olarte, J. M. (2017). Clasificación de movimiento en masa y su distribución en terrenos geológicos de Colombia. https://doi.org/10.32685/9789585978218

Orejuela, I. F. P. (2020). SUSCEPTIBILIDAD a DESLIZAMIENTOS EN LA VÍA ALOAG – SANTO DOMINGO, MEDIANTE LÓGICA DIFUSA. Revista Geoespacial, 17(2), 01-12. https://doi.org/10.24133/geoespacial.v17i2.1571

Oyanguren, P. R., & Monge, L. R. A. (2004). Mecánica de rocas: fundamentos e ingeniería de taludes. En Universidad Privada del Norte. https://oa.upm.es/14183/

Priego, Á., Bocco, G., Mendoza, M., & Garrido, A. (2011). Propuesta para la generación semiautomatizada de unidades de paisaje. Universidad Nacional Autónoma de México. Centro de Investigaciones en Geografía

Ambiental eBooks. https://doi.org/10.22201/ciga.9789688179239p.2011

Quilumba Dután, Diana Liced. (2021). Tomografía Sísmica En La Caracterización de La Mega- Falla Puná-Pallatanga-Cosanga-Chingual. 49 p. http://repositorio.ikiam.edu.ec/jspui/handle/RD_IKIAM/564

Román, A. Q., & Feoli-Boraschi, S. (2018). Comparación de la Metodología Mora-Vahrson y el Método Morfométrico para Determinar Áreas Susceptibles a Deslizamientos en la Microcuenca del Río Macho, Costa Rica. Revista Geográfica de América Central, 1(60). https://doi.org/10.15359/rgac.61-2.1

Saaty, R. (1987). The analytic hierarchy process—what it is and how it is used. Mathematical Modelling, 9(3-5), 161-176. https://doi.org/10.1016/0270-0255(87)90473-8

Salehpour Jam, A., Mosaffaie, J., Sarfaraz, F. et al. GIS-based landslide susceptibility mapping using hybrid MCDM models. Nat Hazards 108, 1025–1046 (2021). https://doi.org/10.1007/s11069-021-04718-5

Sasireka, K., Suribabu, C., & Neelakantan, T. (2019). Extreme Rainfall Return Periods using Gumbel and Gamma Distribution. International Journal Of Recent Technology And Engineering (IJRTE), 8(4S2), 26-29. https://doi.org/10.35940/ijrte.d1007.1284s219

Secretaría Nacional de Gestión de Riesgos. (s. f.). La vía Papallacta-Baeza interrumpido por deslaves. Recuperado de 26 de noviembre del 2024, de https://www.gestionderiesgos.gob.ec/la-via-papallacta-baeza-interrumpido-por-deslaves/

Selby, M. J. (1993). Hillslope Materials and processes. Oxford University Press, 451p.

Servicio Nacional de Gestión de Riesgos y Emergencias (2022). Informe Nro. 136 - Época lluviosa del 01 de enero al 22 de julio de 2022. Inf. téc. Servicio Nacional de Gestión de Riesgos y Emergencias.

Vazquéz Conde, M. T. (2002). El clima en la inestabilidad de laderas: La época de lluvias. In El clima en la inestabilidad de laderas: La época de lluvias (pp. 18-18).

Villón Béjar, M. (2014). HidroEsta, software para cálculos hidrológicos y estadísticos aplicados a la Hidrología. Revista Digital: Matemática, Educación E Internet, 12(2). https://doi.org/10.18845/rdmei.v12i2.1678

Wieczorek, G. F., & Snyder, J. B. (2009). Monitoring slope movements. En Geological Society of America eBooks. https://doi.org/10.1130/2009.monitoring(11)

Wyllie, D.C., & Mah, C. (2004). Rock Slope Engineering: Fourth Edition (4th ed.). CRC Press. https://doi.org/10.1201/9781315274980

Yin, L., Huang, C., Hao, S., Miao, L., Li, J., Qiu, Y., & Liu, H. (2023). Experimental Study on the Stability of Shallow Landslides in Residual Soil. Water, 15(21), 3732. https://doi.org/10.3390/w15213732

Zhang, C., Bai, Q., Han, P. et al. Strength weakening and its micromechanism in water–rock interaction, a short review in laboratory tests. Int J Coal Sci Technol 10, 10 (2023). https://doi.org/10.1007/s40789-023-00569-6